Giant thermal magnetoresistance driven by graphene magnetoplasmon

Ming-Jian He, Hong Qi, Yan-Xiong Su, Ya-Tao Ren, Yi-Jun Zhao, Mauro Antezza

Applied Physics Letters

Giant thermal magnetoresistance driven by graphene magnetoplasmon

Cite as: Appl. Phys. Lett. **117**, 113104 (2020); https://doi.org/10.1063/5.0022261
Submitted: 19 July 2020 . Accepted: 04 September 2020 . Published Online: 16 September 2020

Ming-Jian He, Hong Qi, Yan-Xiong Su, Ya-Tao Ren, Yi-Jun Zhao, and Mauro Antezza

Applied Physics Letters ARTICLE scitation.org/journal/apl

Giant thermal magnetoresistance driven by graphene magnetoplasmon

Cite as: Appl. Phys. Lett. **117**, 113104 (2020); doi: 10.1063/5.0022261
Submitted: 19 July 2020 · Accepted: 4 September 2020 ·
Published Online: 16 September 2020

Ming-Jian He,[1,2] Hong Qi,[1,2,a)] Yan-Xiong Su,[1,2] Ya-Tao Ren,[1,2] Yi-Jun Zhao,[1] and Mauro Antezza[3,4]

AFFILIATIONS

[1]School of Energy Science and Engineering, Harbin Institute of Technology, Harbin 150001, People's Republic of China
[2]Key Laboratory of Aerospace Thermophysics, Ministry of Industry and Information Technology, Harbin 150001, People's Republic of China
[3]Laboratoire Charles Coulomb (L2C), UMR 5221 CNRS-Université de Montpellier, F-34095 Montpellier, France
[4]Institut Universitaire de France, 1 Rue Descartes, F-75231 Paris, France

[a)]**Author to whom correspondence should be addressed:** qihong@hit.edu.cn

ABSTRACT

In this work, we have predicted a giant thermal magnetoresistance for the thermal photon transport based on the tunable magnetoplasmon of graphene. By applying an external magnetic field, we find that the heat flux can be modulated by approximately three orders of magnitude. Accordingly, both negative and giant relative thermal magnetoresistance ratios are achieved for magnetic fields with a maximum strength of 4 Tesla. This effect is mainly caused by the suppression and enhancement of scattering interactions mediated by a graphene magnetoplasmon. Specifically, it has never been achieved before for nanoparticles, which have no response to magnetic fields. The effect is remarkable at these reasonable strengths of fields and, thus, has considerable significance for real-life applications. It is also expected to enable technological advances for thermal measurement-based magnetic sensors and magnetically thermal management.

The giant magnetoresistance effect discovered by Grünberg and Fert in 1988[1] is considered as one of the most fascinating advances in solid state physics. Since then, extensive applications of magnetoresistance have been developed in electronics, such as magnetic sensors and hard-disk read-heads.[2] Inspired by the unique effect, a thermal analog, named the giant thermal magnetoresistance (GTM) effect, is predicted in magneto-optical plasmonic structures in the context of radiative heat transfer.[3] Nowadays, the radiative heat transfer at the nanoscale is of great current interest[4–8] and has highlighted the possibility of modulating heat flux.[9–13] With the application of an external magnetic field, some unique phenomena can be observed in magnetophotonic crystals[14] and magnetoplasmonics.[15,16] Among them, near-complete violation of Kirchhoff's law is observed in the nonreciprocal structure and it provides opportunities in energy harvesting and thermal radiation control.[17,18] The magneto-optical material InSb has shown remarkable performance in modulating the radiative heat transfer due to the magnetically tunable properties.[5,19–23] More recently, by investigating the near-field radiative heat transfer between two InSb particles, a huge anisotropic thermal magnetoresistance with values of up to 800% is achieved with a magnetic field of 5 T.[24] The GTM effect has great application significance for thermal measurement-based magnetic sensing and magnetically thermal management. However, the GTM in plasmonic structures has so far strictly relied on the magneto-optical nanoparticles made of semiconductors, like InSb. The realization of GTM is still demanding for nanoparticle structures made of conventional materials, which has no response to the magnetic field.

By locating a substrate near two nanoparticles, Dong *et al.*[25] have introduced a channel of propagating surface waves to assist the heat transfer. They have delayed the deterioration of thermal photon transport, especially at a long distance. Then, the performance of the long-distance energy exchange was improved by exciting the surface plasmon polaritons of graphene.[8,26] Specifically, in the presence of an external magnetic field, hybridization occurs between cyclotron excitations and plasmons in graphene, originating magnetoplasmon polaritons (MPPs).[27] The MPP effect has been utilized to realize magnetically tunable near-field radiative heat transfer between suspended graphene sheets[28,29] and gratings.[30] In the present work, based on the graphene MPP, we have proposed a scheme to induce a GTM effect between two nanoparticles, made of common materials silicon dioxide (SiO_2). It should be mentioned that the giant thermal magnetoresistance effect obtained in the present work is indeed remarkable and much stronger than those in the previous study.[3]

Here, we consider two SiO_2[31] nanoparticles located above a graphene sheet with a distance z_n, and they are separated by a distance d as illustrated in Fig. 1. The radii of the two nanoparticles are identical and selected as 5 nm, which have been widely used in previous studies.[20,26,32] We limit the calculations with the particle-surface distance of $z_n = 50$ nm and particle-particle distance $d \geq 100$ nm to guarantee the validity of dipolar approximation.[20,26] The two nanoparticles are kept at temperatures T_1 and T_2. A static magnetic field with intensity B is applied perpendicular to the graphene sheet. It should be mentioned that the substrate effect is ignored in the present work to avoid MPP hybridization with other modes. Thus, the pure effect of MPP on the heat transfer mechanism can be distinguished clearly. Moreover, suspended graphene sheets are always considered as ideal physical models for the studies of near-field radiative heat transfer.[11,28,29,33] As illustrated in Fig. 1, the thermal photons transfer through two channels, (1) the direct particle-particle channel via vacuum interaction and (2) the particle-graphene-particle channel via scattering interaction.

With the application of an external magnetic field, a characteristic optical quantum Hall effect occurs to graphene electrons.[34] The conductivity of graphene becomes a tensor with nonzero elements in off diagonal parts,

$$\begin{pmatrix} \sigma_{xx} & \sigma_{xy} \\ \sigma_{yx} & \sigma_{yy} \end{pmatrix} = \begin{pmatrix} \sigma_L & \sigma_H \\ -\sigma_H & \sigma_L \end{pmatrix}, \tag{1}$$

where σ_L and σ_H denote the longitudinal and Hall conductivities, respectively. The magneto-optical conductivities are taken from Refs. 34 and 35, and the chemical potential of graphene is selected as $\mu = 0.08$ eV throughout this letter. The intensity of the magnetic field is limited to $B = 0$–4 T, which has significance for real-life applications. Under this circumstance, the effect of magnetic fields on modifying the optical properties of SiO_2 can be ignored.[36] The violation of Kirchhoff's law in non-reciprocal systems, as demonstrated in Refs. 17 and 18, is not considered in the present work, for the reason that the off diagonal conductivities of magneto-optical graphene result in insignificant nonreciprocity.

Based on the dipole approximation, the electric polarizabilities of the nanoparticles are given by[26]

$$\alpha^{(0)}(\omega) = 4\pi R^3 \frac{\varepsilon(\omega) - 1}{\varepsilon(\omega) + 2}, \tag{2}$$

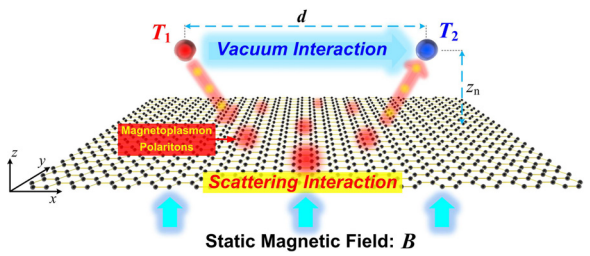

FIG. 1. Schematic of radiative heat transfer between two nanoparticles (separated with a distance d) located above a graphene sheet with a distance z_n. A static magnetic field with intensity B is applied perpendicular to the graphene sheet. There are two channels for energy exchange, (1) the direct particle–particle channel via vacuum interaction and (2) the particle-graphene-particle channel via scattering interaction.

where R and $\varepsilon(\omega)$ are the radius and dielectric function of the nanoparticles, respectively. The polarizability needs to be modified by fluctuation-dissipation theorem,

$$\chi(\omega) = \mathrm{Im}[\alpha(\omega)] - \frac{k_0^3}{6\pi}|\alpha(\omega)|^2, \tag{3}$$

where $\alpha(\omega) = \alpha^{(0)}(\omega)/[1 - i\omega^3\alpha^{(0)}(\omega)/(6\pi c^3)]$ is the dressed polarizability with the radiation correction and $k_0 = \omega/c$.

Then, we introduce the radiative heat transfer in the proposed system. The whole system including the graphene sheet is assumed to be thermalized at $T = T_1 = T_2 = 300$ K in the initial state, and then nanoparticle 1 is heated up to $T_1 = T + \Delta T$. This causes a heat flux $\Delta\varphi$ between the two nanoparticles. It should be mentioned that the graphene sheet also emits thermal radiation, whereas the effect is considered in the scattering interaction. The main point of the present work is to investigate the energy exchange between the two nanoparticles, and thus, the heat transfer between graphene and the nanoparticles is not investigated here. A radiative heat transfer conductance is defined to quantitatively evaluate the heat flux

$$h = \lim_{\Delta T \to 0} \frac{\Delta\varphi}{\Delta T} = 4\int_0^{+\infty} \frac{d\omega}{2\pi} \hbar\omega k_0^4 \frac{\partial n(\omega, T)}{\partial T} \chi^2 \mathrm{Tr}(\mathbf{G}\mathbf{G}^*), \tag{4}$$

where $n(\omega, T) = [\exp(\frac{\hbar\omega}{k_B T}) - 1]^{-1}$ is the Bose-Einstein distribution and $*$ denotes the conjugate transpose. $\mathbf{G}$ is the dyadic Green tensor composed of two parts, i.e., $\mathbf{G} = \mathbf{G}^{(0)} + \mathbf{G}^{(sc)}$. $\mathbf{G}^{(0)}$ and $\mathbf{G}^{(sc)}$ represent the contributions of vacuum and scattering interaction, accounting for direct particle-particle and particle-interface-particle channels, respectively. The two parts read as

$$\mathbf{G}^{(0)} = \frac{e^{ik_0 d}}{4\pi k_0^2 d^3} \begin{pmatrix} a & 0 & 0 \\ 0 & b & 0 \\ 0 & 0 & b \end{pmatrix}, \tag{5a}$$

$$\mathbf{G}^{(sc)} = \int_0^{+\infty} \frac{dk}{2\pi} \frac{ike^{2ik_z z}}{2k_0^2 k_z} (r_s \mathbf{S} + r_p \mathbf{P}), \tag{5b}$$

where $a = 2 - 2ik_0 d$ and $b = k_0^2 d^2 + ik_0 d - 1$. k and $k_z = \sqrt{k_0^2 - k^2}$ are the parallel and perpendicular wave-vectors. More details including the matrices $\mathbf{S}$ and $\mathbf{P}$ can be found in Ref. 26. We note that due to the Hall conductivities, the cross-polarization reflection coefficients r_{sp} and r_{ps} are involved in the reflection characteristics of magneto-optical graphene.[28–30] They do not appear in Eq. (5b), whereas it does not mean that the Hall conductivities play no role in the scattering interaction. In particular, r_s and r_p in Eq. (5b) are modified to take in consideration of the effects of both σ_L and σ_H,[37]

$$r_s = \frac{2\sigma_L Z^h + \eta_0^2(\sigma_L^2 + \sigma_H^2)}{-(2 + Z^h\sigma_L)(2 + Z^e\sigma_L) - \eta_0^2\sigma_H^2}, \tag{6a}$$

$$r_p = \frac{2\sigma_L Z^e + \eta_0^2(\sigma_L^2 + \sigma_H^2)}{(2 + Z^h\sigma_L)(2 + Z^e\sigma_L) + \eta_0^2\sigma_H^2}, \tag{6b}$$

where $Z^h = i\omega\mu_0/k$, $Z^e = ik/\omega\varepsilon_0$, and η_0 denotes the free-space impedance.

A recent experimental study has shown that the radiative heat transfer between two coplanar membranes can be modulated by bringing a third planar object into close proximity.[9] The configuration is similar to the present work. However, with the determined geometric

parameters in the system, the heat flux is fixed. This work presents a scheme for the configuration to dynamically modulate thermal transport using the magnetic method. In Fig. 2(a), for different separation distances d between the two particles, the modulation performance of the magnetic field is demonstrated by the modulation factors $\eta = h(B)/h(0)$ as a function of B. We show that by tuning the intensities of the magnetic fields, the heat transfer can be either enhanced or suppressed compared to that of zero field. The factor η can be tuned nearly over three orders of magnitude with the reasonable strength of fields, $B = 0$–4 T. In addition, we observe a slight oscillation of η emerging at weak fields $B = 0$–0.6 T. To reveal the GTM in the proposed system, a relative thermal magnetoresistance ratio is defined as $R_{TMR} = [R(B)\text{-}R(0)]/R(0) = [h(0)/h(B)\text{-}1] \times 100\%$, where the thermal magnetoresistance is given by $R = 1/h$. As given by the definition, the positive and negative values of R_{TMR} represent the decayed and enhanced heat transport compared to the zero field. It is shown in Fig. 2(a) that at $d = 1556$ nm, R_{TMR} reaches values of up to 635% and low to -83.7% at the fields of $B = 4$ T and 1.17 T, respectively. For $d = 673$ nm, the maximum and minimum of R_{TMR} are achieved at $B = 4$ T and 1.09 T for 7734% and −58.5%, respectively. It should be mentioned that the giant $R_{TMR} = 7734\%$ is much larger than those of previous studies.[3,19,24] Additionally, the negative $R_{TMR} = -83.7\%$ reveals relatively strong enhancement of heat transfer with reasonable strengths of the fields, which are much weaker than those of the existing studies on magnetically tunable radiative heat transfer.[22,28] To make out the heat transfer mechanism accounting for the above GTM, we plot in Fig. 2(b) the scattering ratios defined as $\eta_S = h/h^{(0,0)}$, where $h^{(0,0)}$ denotes the contribution of vacuum interactions in the heat transfer conductance. A horizontal dashed line corresponding to $\eta_S = 1$ is shown in Fig. 2(b), which denotes the circumstance when scattering interactions vanish. The results demonstrate that scattering ratios η_S in Fig. 2(b) and the modulation factors η in Fig. 2(a) exhibit similar variable trends with B. As discussed above, the higher η_S stands for more participation of scattering interaction, which is dominated by the graphene MPP. Despite the slight oscillation at weak fields, the primary trend of η_S decays with B. This phenomenon implies that a transition from scattering enhancement to scattering suppression occurs with the enlarging magnetic fields.

To explore the physical mechanism of the GTM, the radiative heat transfer conductance $h(B, \omega)$ is demonstrated in Fig. 3(a) for $d = 1556$ nm. As investigated in previous studies, the phonon polaritons of SiO_2 are excited in the frequency ranges of 8.67×10^{13}–9.47×10^{13} rad/s and 2.03×10^{14}–2.35×10^{14} rad/s.[8,38] The two branches at the specific frequencies are also observed in Fig. 3(a), whereas they differ from each other sharply in the magnetic-dependent spectrum. The low-frequency branch converts to broadband at weak fields due to the interactions with graphene MPP. Then, as B enhances, this branch is divided into two parts. They correspond to the intraband

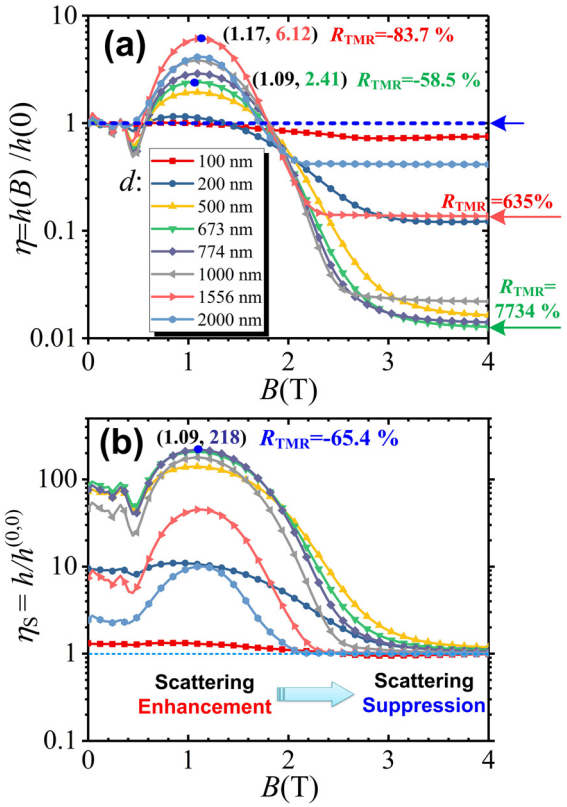

FIG. 2. (a) Modulation factors $\eta = h(B)/h(0)$ together with the relative thermal magnetoresistance ratio $R_{TMR} = [R(B)\text{-}R(0)]/R(0) = [h(0)/h(B)\text{-}1] \times 100\%$. (b) Scattering ratios defined as $\eta_S = h/h^{(0,0)}$, where $h^{(0,0)}$ denotes the contribution of vacuum interactions in the heat transfer conductance.

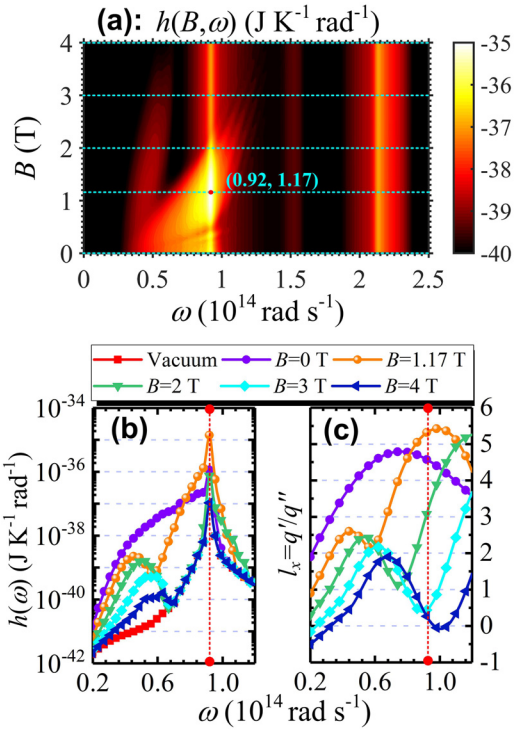

FIG. 3. (a) Radiative heat transfer conductance $h(B, \omega)$ for $d = 1556$ nm. (b) Spectral heat transfer conductance $h(\omega)$ for vacuum interaction and different fields with scattering. (c) Propagating properties of the MPP modes as the reciprocal of localization length in the x direction.

(low-frequency) and the first interband transitions (high-frequency) of graphene MPP,[30,34] respectively. The maximum of $h(B, \omega)$ occurs at $B = 1.17$ T and $\omega = 0.92 \times 10^{14}$ rad/s, where the first interband MPP interacts with low-frequency phonon polaritons of SiO_2 and forms a strong coupling. To gain deep insight into the effect of the strengths of magnetic fields, we plot $h(\omega)$ in Fig. 3(b) corresponding to different cases: (1) the vacuum conductance without graphene and (2) different strengths of fields, which are sliced with dashed lines in Fig. 3(a). The peak value of $h(\omega)$ for $B = 1.17$ T is larger than those of $B = 0$, 2 T and $B = 3$, 4 T by approximately one and two orders of magnitude. We can infer that this enhancement of $h(\omega)$ leads to $R_{TMR} = -83.7\%$ in Fig. 2(a). In addition, we find that as B enhances and exceeds 3 T, the intraband MPP almost fades out and the interband MPP decouples with phonon polaritons of SiO_2. This results in the decaying trend of $h(\omega)$ with B, and $h(\omega)$ nearly reduces to that of vacuum interaction with $B > 3$ T. The above results imply that the evolution of the MPP modes with magnetic fields plays a crucial role in GTM. Therefore, in Fig. 3(c), we demonstrate the propagating properties of the MPP modes. They are given by the reciprocal of the localization length in the x direction, defined as $l_x = q'/q''$.[27] q' and q'' represent the real and imaginary parts of the complex longitudinal wave vector, respectively. A red dashed line is added in Fig. 3(c), indicating the same frequency as that in Fig. 3(b). The different peak values of $h(\omega)$ can be well explained by the magnitudes of l_x. We can confirm that the MPP modulates the scattering interactions based on the strong dependence of the propagating length on the intensities of magnetic fields.

To have an intuitive understanding of the scattering characteristics, in Fig. 4(a), the electric field energy density u_e[25] is illustrated in the x-y plane ($z = z_n/2$) for $\omega = 0.92 \times 10^{14}$ rad/s, corresponding to the peak in Fig. 3(b). u_e values of $B = 4$ T are considerably weakened compared to those of zero field and $B = 1.17$ T. In addition, compared to zero field, u_e has enhanced when a magnetic field $B = 1.17$ T is applied. In Figs. 4(b) and 4(c), the ratios of u_e in $B = 1.17$ T and $B = 4$ T to that in zero field are demonstrated in the x-z plane. The two

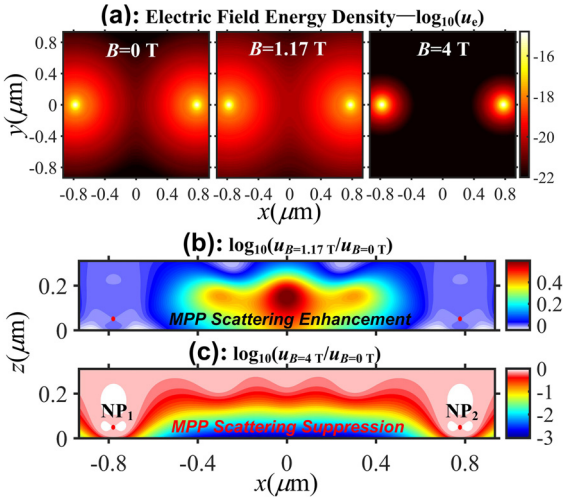

FIG. 4. (a) Electric field energy density u_e in the x-y plane ($z = z_n/2$) for $\omega = 0.92 \times 10^{14}$ rad/s. Ratio of u_e in (b) $B = 1.17$ T and (c) $B = 4$ T to that in zero field in the x-z plane. The two nanoparticles are indicated by red spots near $x = \pm 0.8$ μm.

nanoparticles are indicated by red spots near $x = \pm 0.8$ μm. The positive and negative ratios represent the enhancement and suppression of u_e. A scattering enhancement occurs in Fig. 4(b) between the two nanoparticles, and it is concentrated above graphene with a distance of $z \approx 1.5$ μm. Interestingly, the strongest enhancement locates away from the graphene surface and even higher than the nanoparticles. It should be pointed out that the electric field energy density remains confined near the graphene surface at different magnetic fields. The enhancement is demonstrated by the ratio of u_e distribution at different fields compared to zero field. As is known, the surface plasmon polaritons of graphene are always excited and confined near the interface,[27] and it is the same as the scattering enhancement by graphene.[8] The unique scattering enhancement at this position has never been observed in graphene plasmons before. The enhancement, which is far away from the interface, is mainly caused by the considerable difference between the surface plasmon modes in the absence and presence of magnetic fields. The MPP modes at $B = 1.17$ T have a greater ability to assist the heat transfer than the surface plasmon polaritons at zero modes, especially at this location. Specifically, a remarkable scattering suppression is observed in Fig. 4(c) near the graphene sheet. The $B = 4$ T field shuts off the energy-exchange channel dominated by graphene, and thus, an attenuation works on the heat flux between the particles. Then, we can conclude from the above results that the negative and giant thermal magnetoresistance effects are attributed to the MPP scattering enhancement and MPP scattering suppression, respectively.

In summary, we have predicted a negative and a giant thermal magnetoresistance effect between two SiO_2 nanoparticles based on the graphene MPP. The relative thermal magnetoresistance ratio can reach values of up to 7734% and low to −83.7% for magnetic fields of 4 T and 1.17 T, respectively. These values are indeed remarkable at these strengths of fields and have never been achieved in nanoparticle structures made of conventional materials, which has no response to the magnetic field. We show that this behavior mainly results from the suppression and enhancement of scattering interaction mediated by graphene MPP. The effect in the present work is promising for thermal measurement-based magnetic sensing and magnetically thermal management. The physics in this work is limited to the fixed chemical potentials of graphene and geometry sizes (R, z_n). However, it does not mean that the GTM obtained in this work is a special case. By applying different properties of graphene and nanoparticles, different magnitudes and even much greater GTM effects can be predicted. The prediction in this work is universal, and we believe that the optimized parameters can result in a more considerable GTM effect. Moreover, we expect in the future work that magneto-optical materials like InSb can act as the substrate and assist in the GTM.

The support of this work by the National Natural Science Foundation of China (Nos. 51976044 and 51806047) is gratefully acknowledged. The Heilongjiang Touyan Innovation Team Program is gratefully acknowledged. M.A. acknowledges support from the Institute Universitaire de France, Paris, France (UE).

DATA AVAILABILITY

The data that support the findings of this study are available from the corresponding author upon reasonable request.

REFERENCES

[1]M. N. Baibich, "Giant magnetoresistance of Fe/Cr magnetic superlattices," Phys. Rev. Lett. **61**, 2472 (1988).
[2]I. Ennen, D. Kappe, T. Rempel, C. Glenske, and A. Hütten, "Giant magnetoresistance: Basic concepts, microstructure, magnetic interactions and applications," Sensors **16**(6), 904 (2016).
[3]I. Latella and P. Ben-Abdallah, "Giant thermal magnetoresistance in plasmonic structures," Phys. Rev. Lett. **118**(17), 173902 (2017).
[4]J. C. Cuevas and F. J. García-Vidal, "Radiative heat transfer," ACS Photonics **5**(10), 3896–3915 (2018).
[5]P. Benabdallah, "Photon thermal Hall effect," Phys. Rev. Lett. **116**(8), 084301 (2016).
[6]S. A. Biehs, F. S. S. Rosa, and P. Ben-Abdallah, "Modulation of near-field heat transfer between two gratings," Appl. Phys. Lett. **98**(24), 243102 (2011).
[7]X. L. Liu and Z. M. Zhang, "Giant enhancement of nanoscale thermal radiation based on hyperbolic graphene plasmons," Appl. Phys. Lett. **107**(14), 143114 (2015).
[8]M.-J. He, H. Qi, Y.-T. Ren, Y.-J. Zhao, and M. Antezza, "Graphene-based thermal repeater," Appl. Phys. Lett. **115**(26), 263101 (2019).
[9]D. Thompson, L. Zhu, E. Meyhofer, and P. Reddy, "Nanoscale radiative thermal switching via multi-body effects," Nat. Nanotechnol. **15**(2), 99–104 (2020).
[10]H. Iizuka and S. Fan, "Significant enhancement of near-field electromagnetic heat transfer in a multilayer structure through multiple surface-states coupling," Phys. Rev. Lett. **120**(6), 063901 (2018).
[11]P. Benabdallah, A. Belarouci, L. Frechette, and S. A. Biehs, "Heat flux splitter for near-field thermal radiation," Appl. Phys. Lett. **107**(5), 053109 (2015).
[12]S. Basu and M. Francoeur, "Near-field radiative transfer based thermal rectification using doped silicon," Appl. Phys. Lett. **98**(11), 113106 (2011).
[13]M. He, H. Qi, Y. Ren, Y. Zhao, and M. Antezza, "Active control of near-field radiative heat transfer by a graphene-gratings coating-twisting method," Opt. Lett. **45**(10), 2914 (2020).
[14]M. Vanwolleghem, X. Checoury, W. Smigaj, B. Gralak, L. Magdenko, K. Postava, B. Dagens, P. Beauvillain, and J. M. Lourtioz, "Unidirectional band gaps in uniformly magnetized two-dimensional magnetophotonic crystals," Phys. Rev. B **80**(12), 121102(R) (2009).
[15]L. Halagačka, M. Vanwolleghem, F. Vaurette, J. Ben Youssef, K. Postava, J. Pištora, and B. Dagens, "Magnetoplasmonic nanograting geometry enables optical nonreciprocity sign control," Opt. Express **26**(24), 31554 (2018).
[16]L. Halagačka, M. Vanwolleghem, K. Postava, B. Dagens, and J. Pištora, "Coupled mode enhanced giant magnetoplasmonics transverse Kerr effect," Opt. Express **21**(19), 21741 (2013).
[17]B. Zhao, Y. Shi, J. Wang, Z. Zhao, N. Zhao, and S. Fan, "Near-complete violation of Kirchhoff's law of thermal radiation with a 0.3 T magnetic field," Opt. Lett. **44**(17), 4203–4206 (2019).
[18]L. Zhu and S. Fan, "Near-complete violation of detailed balance in thermal radiation," Phys. Rev. B **90**(22), 220301(R) (2014).
[19]E. Moncada-Villa, V. Fernández-Hurtado, F. J. García-Vidal, A. García-Martín, and J. C. Cuevas, "Magnetic field control of near-field radiative heat transfer and the realization of highly tunable hyperbolic thermal emitters," Phys. Rev. B **92**(12), 125418 (2015).
[20]A. Ott, R. Messina, P. Ben-Abdallah, and S.-A. Biehs, "Radiative thermal diode driven by nonreciprocal surface waves," Appl. Phys. Lett. **114**(16), 163105 (2019).
[21]A. Ott and S.-A. Biehs, "Thermal rectification and spin-spin coupling of nonreciprocal localized and surface modes," Phys. Rev. B **101**, 155428 (2020).
[22]J. Song, Q. Cheng, L. Lu, B. Li, K. Zhou, B. Zhang, Z. Luo, and X. Zhou, "Magnetically tunable near-field radiative heat transfer in hyperbolic metamaterials," Phys. Rev. Appl. **13**(2), 024054 (2020).
[23]C. Guo, Y. Guo, and S. Fan, "Relation between photon thermal Hall effect and persistent heat current in nonreciprocal radiative heat transfer," Phys. Rev. B **100**(20), 205416 (2019).
[24]R. M. Abraham Ekeroth, P. Ben-Abdallah, J. C. Cuevas, and A. García-Martín, "Anisotropic thermal magnetoresistance for an active control of radiative heat transfer," ACS Photonics **5**(3), 705–710 (2018).
[25]J. Dong, J. Zhao, and L. Liu, "Long-distance near-field energy transport via propagating surface waves," Phys. Rev. B **97**(7), 075422 (2018).
[26]R. Messina, S.-A. Biehs, and P. Ben-Abdallah, "Surface-mode-assisted amplification of radiative heat transfer between nanoparticles," Phys. Rev. B **97**(16), 165437 (2018).
[27]A. Ferreira, N. M. R. Peres, and A. H. Castro Neto, "Confined magneto-optical waves in graphene," Phys. Rev. B **85**(20), 205426 (2012).
[28]H. Wu, Y. Huang, L. Cui, and K. Zhu, "Active magneto-optical control of near-field radiative heat transfer between graphene sheets," Phys. Rev. Appl. **11**(5), 054020 (2019).
[29]L. Ge, K. Gong, Y. Cang, Y. Luo, X. Shi, and Y. Wu, "Magnetically tunable multiband near-field radiative heat transfer between two graphene sheets," Phys. Rev. B **100**(3), 035414 (2019).
[30]M.-J. He, H. Qi, Y.-T. Ren, Y.-J. Zhao, and M. Antezza, "Magnetoplasmonic manipulation of nanoscale thermal radiation using twisted graphene gratings," Int. J. Heat Mass Transfer **150**, 119305 (2020).
[31]E. D. Palik, *Handbook of Optical Constants of Solids II* (Boston Academic Press, 1991), Vol. 1, pp. 77–135.
[32]Y. Zhang, M. Antezza, H. L. Yi, and H. P. Tan, "Metasurface-mediated anisotropic radiative heat transfer between nanoparticles," Phys. Rev. B **100**, 085426 (2019).
[33]M.-J. He, H. Qi, Y.-F. Wang, Y.-T. Ren, W.-H. Cai, and L.-M. Ruan, "Near-field radiative heat transfer in multilayered graphene system considering equilibrium temperature distribution," Opt. Express **27**(16), A953 (2019).
[34]V. P. Gusynin, S. G. Sharapov, and J. P. Carbotte, "Magneto-optical conductivity in graphene," J. Phys.: Condens. Matter **19**(2), 026222 (2007).
[35]A. Ferreira, J. Viana-Gomes, Y. V. Bludov, V. Pereira, N. M. R. Peres, and A. H. Castro Neto, "Faraday effect in graphene enclosed in an optical cavity and the equation of motion method for the study of magneto-optical transport in solids," Phys. Rev. B **84**(23), 235410 (2011).
[36]Y. Zhang, Y.-W. Tan, H. L. Stormer, and P. Kim, "Experimental observation of the quantum Hall effect and Berry's phase in graphene," Nature **438**(7065), 201–204 (2005).
[37]T. Cysne, W. J. M. Kort-Kamp, D. Oliver, F. A. Pinheiro, F. S. S. Rosa, and C. Farina, "Tuning the Casimir-Polder interaction via magneto-optical effects in graphene," Phys. Rev. A **90**(5), 052511 (2014).
[38]M.-J. He, H. Qi, Y. Li, Y.-T. Ren, W.-H. Cai, and L.-M. Ruan, "Graphene-mediated near field thermostat based on three-body photon tunneling," Int. J. Heat Mass Transfer **137**, 12–19 (2019).